Mechanical signaling via nonlinear wavefront propagation in a mechanically excitable medium

Timon Idema[1,2,*] and Andrea J. Liu[1,†]

[1]*Department of Physics and Astronomy, University of Pennsylvania, Philadelphia, Pennsylvania, USA*

[2]*Department of Bionanoscience, Kavli Institute of Nanoscience, Faculty of Applied Sciences, Delft University of Technology, Delft, The Netherlands*

(Received 5 April 2013; published 23 June 2014)

Models that invoke nonlinear wavefront propagation in a chemically excitable medium are rife in the biological literature. Indeed, the idea that wavefront propagation can serve as a signaling mechanism has often been invoked to explain synchronization of developmental processes. In this paper we suggest a kind of signaling based not on diffusion of a chemical species but on the propagation of mechanical stress. We construct a theoretical approach to describe mechanical signaling as a nonlinear wavefront propagation problem and study its dependence on key variables such as the effective elasticity and damping of the medium.

DOI: 10.1103/PhysRevE.89.062709 PACS number(s): 87.17.Aa, 87.53.Ay

I. INTRODUCTION

The physical phenomenon of nonlinear wavefront propagation in an excitable medium is widely exploited by biological systems to transmit signals across many cells. For example, when the slime mold *Dictyostelium* begins to aggregate to form a fruiting body, wavefronts of the molecule cAMP propagate across the amoeba colony [1–3]. Although cAMP itself spreads diffusively, wavefronts of cAMP propagate ballistically across the amoeba colony because the colony is chemically excitable: when the local concentration of cAMP exceeds a threshold, further local release of the species is triggered [2,3]. Similar wavefronts of calcium and potassium, respectively, signal fertilization in eggs [4] and the onset of spreading cortical depression [5], associated with migraine auras.

Biological systems are typically overdamped, so they do not support sound waves and stress cannot propagate ballistically. In this paper we consider the possibility that mechanical signaling via ballistic propagation of a nonlinear wavefront can occur in a mechanically excitable medium, much as chemical signaling via ballistic propagation of a nonlinear wavefront can occur in a chemically excitable medium. In recent years there has been a growing recognition that mechanics plays an important role in biology, and that many cells sense and respond not only to chemical stimuli but also to mechanical stimuli [6–10]. This raises the possibility that mechanosensing at the cellular level could give rise to collective phenomena at larger length scales, such as collective cell migration [11,12]. In this paper, we consider models in which mechanosensing causes cells, or components of cells, to *deform*, thus generating more stress. We show that this nonlinear response to stress can lead to mechanically induced nonlinear wavefront propagation—a particular form of mechanical signaling—at the tissue level.

Several groups have previously studied waves in active matter [11,13–22]. For instance, Günther and Kruse showed how spontaneous oscillations in muscle fibers can lead to propagating waves in an overdamped viscoelastic medium which by itself is linearly stable [15,16]. Both Banerjee and Marchetti [17,18] and Radszuweit *et al.* [19] have studied the dynamics of viscoelastic polymer gels that can be contracted by molecular motors, and shown that the addition of motor dynamics to the overdamped system can lead to ballistic waves. Recently, Köpf and Pismen showed that combining the properties of a polarizable, nonlinear elastic medium and chemo-mechanical coupling can lead to nonlinear instabilities as well, and be used to explain the properties of growing epithelial tissue [20]. Building on this work, they also showed that a similar model can lead to both long-wave and short-wave instabilities and pattern formation [21]. In contrast to these previous studies, where activity occurs continuously in space and time, we consider models of a different class of active matter, in which activity in the form of stress generation is localized to *discrete* positions in space and occurs only when *activated* by stress. We consider both overdamped elastic systems and viscoelastic systems, neither of which allow for the propagation of ballistic waves. Because we add activity only to discrete points, our approach allows us to directly relate the observable properties of the emerging waves to those of the underlying (visco)elastic medium.

It has recently been suggested that two very different biological systems might be mechanically excitable in this sense: the early *Drosophila* embryo [23] and the developing heart [24]. The early *Drosophila* embryo supports mitotic wavefronts: nuclei at the poles of the embryo tend to divide first, giving rise to a mitotic wavefront separating dividing nuclei from those that have not yet divided. This wavefront propagates across the entire embryo [25] at constant speed [23]. Likewise, the heart tube of the avian embryo beats via contractile wavefronts that are initiated at one end of the tissue and propagate across the heart tube with each beat [26]. These two examples differ completely in their biological details but are both described at a quantitative level by models [23,24] that assume that mechanosensing leads to the generation of more stress. In these systems, the active agents (the nuclei and cells) are discrete points which are separated by a passive medium. Therefore the existing models, which describe continuum active systems such as molecular motors distributed throughout a (visco)elastic gel, do not directly apply. It is therefore important to construct minimal models of mechanically excitable media and to understand their behavior more generally.

*t.idema@tudelft.nl

†ajliu@physics.upenn.edu

II. MODELS

We consider two minimal models of mechanically excitable media. In each case, stress can be generated at certain sites, or activatable nodes, if the local stress exceeds some threshold value. In the case of the early *Drosophila* embryo, these nodes would represent cell nuclei, while in the case of the developing heart tube, the nodes would represent cardiomyocytes (heart cells that can contract). In our models, the activatable nodes are embedded in a passive medium that supports mechanical stress and is overdamped. The nodes communicate with each other through this damped elastic medium: when a node is activated and stress is generated, it is transmitted through the medium, potentially causing further activation of other nodes. We solve these models and identify characteristic features exhibited by nonlinear wavefronts in such systems.

We start by considering two simple examples of the passive medium in which the activatable nodes are embedded. The elasticity of the medium is characterized by Lamé coefficients λ and μ, or equivalently, by the Young's modulus E and dimensionless Poisson ratio ν within linear elasticity theory [27]. These parameters relate the stress σ_{ij} inside the elastic material to its strain (deformation) ε_{ij}:

$$\sigma_{ij} = \frac{E}{1+\nu}\left[\varepsilon_{ij} + \frac{\nu}{1-(d-1)\nu}\varepsilon_{kk}\delta_{ij}\right], \tag{1}$$

where d is the number of dimensions (2 or 3), and summation over repeated indices is implied. The strain ε_{ij} is defined in terms of the displacement vector u_i of the elastic material: $\varepsilon_{ij} = \frac{1}{2}(\partial_j u_i + \partial_i u_j)$. To avoid confusion we will follow the usual convention and label the two-dimensional versions of the parameters with a subscript 2; they are related to their three-dimensional counterparts by $E_2 = E/(1-\nu^2)$ and $\nu_2 = \nu/(1-\nu)$ [27]. The force per unit area is given by the divergence of the stress: $P_i = \partial_j \sigma_{ij}$.

In the simplest model that we consider, corresponding to a thin elastic film that slides frictionally over a surface, we balance the elastic force with a friction term $\Gamma \partial_t u_i$, where Γ is the friction coefficient. Such a system can be described by a two-dimensional model with the equation of motion:

$$\Gamma \partial_t u_i = \frac{E_2}{2(1+\nu_2)}\left[\partial_j\partial_j u_i + \frac{1}{1-\nu_2}\partial_i\partial_j u_j\right]. \tag{2}$$

Note that Eq. (2), which describes the response of elastic medium to a displacement u_i, is similar to the diffusion equation, but is a tensor equation instead of a scalar one. Mathematically, this model is the two-dimensional version of the overdamped limit of the viscoelastic gel model first introduced by Tanaka *et al.* [28].

The second model that we consider is a three-dimensional realization of an overdamped elastic medium, such as a polymer network immersed in a fluid. The elasticity of the system is also described by Eq. (1), but the friction force is proportional to the relative motion of the fluid and the elastic network: $\Gamma(\partial_t u_i - v_i)$, where v_i is the fluid velocity. The stress in an incompressible fluid depends linearly on the pressure p and the shear rate, $\dot{\gamma}_{ij}^{\text{visc}} = \frac{1}{2}(\partial_i v_j + \partial_j v_i)$:

$$\sigma_{ij}^{\text{visc}} = -p\delta_{ij} + 2\eta\dot{\gamma}_{ij}^{\text{visc}}, \tag{3}$$

in both two and three dimensions [29]. In the overdamped limit (zero Reynolds number), taking the divergence of (3) gives the Stokes equation. Combining the elastic and fluid equations gives a closed system for u_i, v_i, and p:

$$\Gamma(\partial_t u_i - v_i) = \frac{E}{2(1+\nu)}\left[\partial_j\partial_j u_i + \frac{1}{1-(d-1)\nu}\partial_i\partial_k u_k\right], \tag{4}$$

$$\Gamma(\partial_t u_i - v_i) = \partial_i p - \eta\partial_j\partial_j v_i, \tag{5}$$

$$0 = \partial_j v_j. \tag{6}$$

Equations (4)–(6) are identical to the two-fluid model studied by Levine and Lubensky [30], but without the inertial terms.

We now add mechanical excitability as follows. We consider a collection of nodes at positions $\{\vec{R}_n\}$, where n indexes the nodes. A node can be activated if some measure of the stress (for example, the absolute value of its largest eigenvalue) exceeds a threshold value α. If this occurs at time t, the node releases additional stress over a time interval Δt. For a node at $\vec{R}_n$ activated at time $t = t_n$, we therefore introduce an extra force into Eq. (2), of the form

$$P_i^{\text{active}} = \partial_j[Q_{ij}\delta(\vec{x} - \vec{R}_n)\Theta(t - t_n)\Theta(t_n + \Delta t - t)]. \tag{7}$$

Here $Q_{ij} = f_i x_j + x_i f_j$ is a symmetric tensor of rank 2, corresponding to a force per unit volume $\vec{f}$ acting over a distance $\vec{x}$. Q_{ij} is therefore the symmetric combination of a force and a distance, with the dimensions of a stress (force per unit area), so it represents a stress source. In two dimensions, $Q_{ij} = Q_0\delta_{ij} + Q_1(n_i n_j - \frac{1}{2}\delta_{ij})$ has an isotropic part of the form $Q_0\delta_{ij}$ and a traceless anisotropic part of the form $Q_1(n_i n_j - \frac{1}{2}\delta_{ij})$, where $\hat{n}$ indicates the anisotropy direction. The anisotropic contribution corresponds to a force dipole. In three dimensions, Q_{ij} has a similar isotropic part and two anisotropic parts that together span the plane perpendicular to the anisotropy direction. In general, we could also consider asymmetric contributions to Q_{ij}, which would correspond to torques (one in two dimensions and three in three dimensions).

We solve for the response of the two-dimensional overdamped elastic medium of Eq. (2) to the active force in Eq. (7) by deriving the Green's tensor $G_{ijk}(\vec{x},t)$, which relates the displacement $u_k(\vec{x},t)$ to a source term $Q_{ij}\delta(\vec{x})\Theta(t)$ at the origin at time $t = 0$. We find that the material parameters E_2, ν_2, and Γ combine in two quantities with the dimensions of diffusion constants,

$$D_1 = \frac{E_2}{(1-\nu_2^2)\Gamma} = \frac{2}{1-\nu_2}\frac{\mu}{\Gamma}, \tag{8}$$

$$D_2 = \frac{E_2}{2(1+\nu_2)\Gamma} = \frac{\mu}{\Gamma}, \tag{9}$$

which correspond to motion in the longitudinal and transverse directions, respectively, and together completely determine the solution. Here $\mu = E_2/2(1+\nu_2) = E/2(1+\nu)$ is the material's shear modulus, which is the same in two and three dimensions. The resulting Green's tensor is given in Eq. (A1).

We can derive a similar solution for the response of the two-fluid model of Eqs. (4)–(6) to the active force in Eq. (7). In this case there is an extra parameter, the viscosity η of the fluid,

which gives rise to a natural relaxation timescale $\tau = \mu/\eta$ of the system. In three dimensions, the three quantities governing the solution of Eqs. (4)–(6) are given by

$$D_1 = \frac{E}{\Gamma}\frac{1-\nu}{(1+\nu)(1-2\nu)} = \frac{2(1-\nu)}{1-2\nu}\frac{\mu}{\Gamma}, \tag{10}$$

$$D_2 = \frac{E}{\Gamma}\frac{1}{2(1+\nu)} = \frac{\mu}{\Gamma}, \tag{11}$$

$$\tau = \frac{E}{2\eta(1+\nu)} = \frac{\mu}{\eta}. \tag{12}$$

The associated Green's tensor is given by Eq. (A2).

III. RESULTS

Because the equations governing the passive medium are linear, we can now use the principle of superposition to study the effect of many source terms. We initialize the system by activating a single node at the origin at $t = 0$. We then measure the stress at the other nodes as a function of time, and activate them if they are above threshold by releasing more stress, according to Eq. (7). We consider various cases for the arrangement of the nodes: a regular triangular lattice, a random configuration with short-range correlations (as in a random packing of disks), and an uncorrelated random configuration. In addition, we look at variants in which the force term is purely isotropic (hydrostatic expansion/contraction) or is in the form of a volume-conserving force dipole, with either random orientation or orientations correlated to the direction of the traveling wavefront. In all cases, the model produces an activation wavefront with a well-defined speed, as shown in Fig. 1. We find that the speed of the wavefront depends on the density of nodes but is insensitive to their arrangement. However, the spread of the wavefront around its mean increases with the amount of randomness [Fig. 1(b)]. Not surprisingly, if the orientations of the force dipoles are chosen

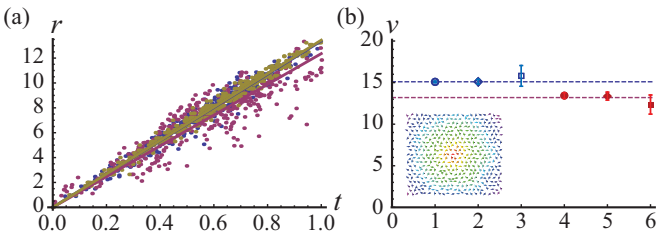

FIG. 1. (Color online) Calculated wavefronts. (a) Plots showing for each node (dots) the distance from the first activated node vs time of activation, with linear fits. This example has a traceless dipole source term ($Q_0 = 0$) and shows results for three different types of grids, all with the same density: regular triangular (gold), correlated random (blue), and uncorrelated random (red). (b) Mean wavefront speed for six realizations, with isotropic force term (1–3, blue, $Q_1 = 0$) and dipole force terms (4–6, red, $Q_0 = 0$), and on three different grids: regular triangular (circle, 1 and 4), correlated random (diamond, 2 and 5), and uncorrelated random (square, 3 and 6). Error bars indicate standard deviations. Inset shows the two-dimensional field of nodes, indicating the orientation in which nodes are activated, and color coded according to the time at which they are activated, on a hue scale (red-yellow-green-blue-violet).

at random, the speed of the wavefront is the same in all directions so that its shape is circular, as in the inset of Fig. 1(b). In contrast, if the dipoles are all oriented in the same direction, the wavefront is no longer uniform but is faster in the direction of orientation. Also, for the same magnitude of the active force, the speed of the wavefront is somewhat higher if the force dipole Q_{ij} is isotropic ($Q_1 = 0$) than if it is a traceless force dipole [$Q_0 = 0$, Fig. 1(b)]. All these observations indicate that the wavefront speed is dictated primarily by the properties of the medium and the average distance between nodes, and is insensitive to both the form of the active force and spatial arrangement of nodes.

Dimensional analysis of the material parameters of our two-dimensional model [Eq. (2)] shows that there is only one possible scaling for the wavefront speed with the material parameters: $v \sim E_2/(a\Gamma)$, where a is the grid spacing. The dimensionless speed $\bar{v} = (a\Gamma/E_2)v$ depends on the material's Poisson ratio ν_2 and the dimensionless threshold $\bar{\alpha} = \alpha a^2/Q$, where Q is the strength of the force term. We have determined the function $\bar{v}(\nu_2, \bar{\alpha})$ numerically for both isotropic and dipole force terms. We find that it obeys a fairly simple functional form, which can be motivated by an analytical argument based on the case of the simplest force term, the purely isotropic one ($Q_1 = 0$, so $Q_{ij} = Q_0\delta_{ij}$). In this case, the stress is given by

$$\sigma_{kl}^{\mathrm{iso}} = \frac{(1-\nu_2)Q_0}{x^2}e^{-x^2/4D_1t} \times \left[\left(2 + \frac{x^2}{2D_1t}\right)\frac{x_k x_l}{x^2} + \left(\frac{\nu_2}{1-\nu_2}\frac{x^2}{2D_1t} - 1\right)\delta_{kl}\right]. \tag{13}$$

Because the stress drops off quadratically with distance, the major contribution to the stress at any node is due to forces exerted by neighboring nodes. Moreover, since the front expands radially, typically only a single nearest neighbor of any node will have been activated recently. We can therefore get a reasonable estimate for the local stress at a node by considering that nearest neighbor to be the only source. We introduce the dimensionless time $\bar{t} = E_2 t/(a^2\Gamma)$; then for a single source a distance a away, the time at which the largest eigenvalue of the stress reaches the dimensionless threshold $\bar{\alpha}$ is given by

$$\bar{\alpha} = (1-\nu_2)\left[1 + \frac{1+\nu_2}{2\bar{t}}\right]e^{-(1-\nu_2^2)/4\bar{t}}. \tag{14}$$

Unfortunately, Eq. (14) cannot be inverted analytically. However, the two factors containing $\bar{t}$ are easily inverted, allowing us to make an educated guess for the functional form of the resulting dimensionless speed:

$$\bar{v} = -\frac{4(c_1\bar{\alpha} + c_2)\log(\bar{\alpha})}{1-\nu_2^2}, \tag{15}$$

where c_1 and c_2 need to be determined numerically; we find $c_1 = 4.0$ and $c_2 = 1.5$. As shown in Fig. 2(a), the form given by Eq. (15) works remarkably well. Moreover, the same functional form also describes the results for a dipole force term wavefront, as shown in Fig. 2(b), the only difference being the values of the two fit parameters—here we find $c_1 = -1.0$ and $c_2 = 1.0$.

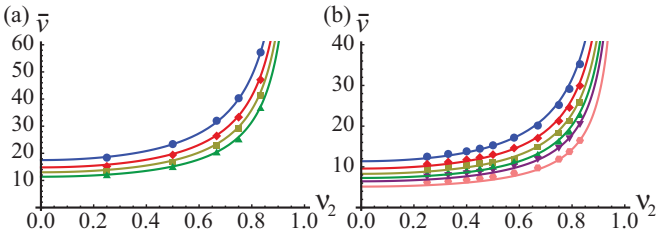

FIG. 2. (Color online) Dimensionless wavefront speed as a function of the Poisson ratio ν_2 and dimensionless threshold $\bar{\alpha}$. Symbols indicate numerical solutions of the full system, lines the functional form of Eq. (15). (a) Isotropic force term $Q_{ij} = Q\delta_{ij}$. Fit parameters $c_1 = 4.0$, $c_2 = 1.5$. Values of $\bar{\alpha}$: 0.1 (blue/dots), 0.2 (red/ diamonds), 0.3 (gold/squares) and 0.4 (green/triangles). (b) Dipole force term with random orientation angle θ: $Q_{ij} = -Q\cos(2\theta)(\delta_{i1}\delta_{j1} - \delta_{i2}\delta_{j2}) - Q\sin(2\theta)(\delta_{i1}\delta_{j2} + \delta_{i2}\delta_{j1})$. Fit parameters $c_1 = -1.0$, $c_2 = 1.0$. Values of $\bar{\alpha}$: 0.050 (blue/dots), 0.075 (red/diamonds), 0.100 (gold/squares), 0.125 (green/triangles up), 0.150 (purple/triangles down), and 0.200 (pink/hexagons).

In line with intuition, our model predicts that there is a maximum threshold value $\bar{\alpha}_{\max}$ above which a wavefront will not propagate. This can happen for one of two reasons: either the force is not large enough to create a stress at the next node that exceeds the threshold value, or the nodes are so far apart that, due to the diffusive nature of the stress spreading, the threshold value is not reached. Both possibilities are contained in the form of the dimensionless version of $\bar{\alpha}_{\max}$, given by the maximum of the right-hand side of Eq. (14), which gives $\bar{\alpha}_{\max} = 2e^{-(1+\nu_2)/2}$ at $\bar{r}_{\max} = \frac{1}{2}(1-\nu_2)$ and corresponding to a minimum speed $\bar{v}_{\min} = 2/(1-\nu_2)$. We note that as ν_2 approaches its maximum value of 1, the minimum speed diverges, as can be seen in Fig. 2(a).

For the three-dimensional two-fluid model of Eqs. (4)–(6), there are two independent quantities with the dimensions of speed, $E/a\Gamma$ and a/τ, where $\tau = \eta/\mu$ is the material's relaxation time [Eq. (12)]. We note that both of these scale linearly with the material's Young's modulus E (or equivalently, with the material's shear modulus μ), which implies that also in this case the resulting wavefront velocity in a similar setup with excitable nodes will scale linearly with that modulus. It will also scale with $\Gamma^{-n}\eta^{1-n}$, where n is some number between 0 and 1, indicating that both the internal viscosity of the moving fluid and the friction between the elastic and viscous material contribute to the damping of the ballistic motion.

In both of our minimal models, the speed of the wavefront scales linearly with the elastic moduli. This distinguishes these wavefronts from ordinary elastic waves, where the speed of the wave scales as the square root of the elastic moduli, as in ordinary sound waves. We emphasize that this distinction stems from the fact that the wavefronts in our models are nonlinear phenomena, distinct from elastic waves.

IV. SUMMARY AND DISCUSSION

In this paper, we have introduced two theoretical realizations of a mechanical signaling mechanism. We have shown that nonlinear wavefront propagation is a robust feature of both models. In both cases, the wavefront velocity is insensitive to the spatial distribution of excitable nodes. It is also insensitive to whether the stress is released in an isotropic or traceless anisotropic fashion. Furthermore, a fundamental feature of both models is that the wavefront velocity is proportional to the Young's modulus of the medium, and the magnitude of the velocity can be understood simply and quantitatively in terms of characteristic dimensionless variables, such as the stress threshold made dimensionless with the magnitude of the force dipole released when a node is excited. We note that the linear scaling of the wavefront propagation speed with the medium's Young's modulus is a direct consequence of the fact that in our model the wave propagates through a passive, mechanical medium, in contrast to propagation through an active gel.

The overdamped elastic models considered here are the simplest models that could be used to describe a tissue. It would be worthwhile to explore mechanical signaling in other models that have been proposed for tissues, including the active gel model [11,13–21] and cellular models [31,32]. The active gel model first proposed by Kruse *et al.* [13,14] is an extension of the two-fluid model of Levine and Lubensky [30] with a continually active (energy-consuming) term to model the dynamics of the cytoskeleton due to motor activity. As we have shown here, such a continuous activity is not necessary to describe wavefront propagation, as local and discrete activity is sufficient. However, given the presence of active motors in the cytoskeleton, it would be interesting to see how the wavefront is affected by an active term in the model. It would also be interesting to compare the results of such an interaction with those of Bois *et al.,* who study pattern formation in active fluids due to chemical signaling [11]. These active models, and the one we used here, are continuous models. However, tissues are, of course, composed of discrete units, the cells. As shown by Manning *et al.,* several mechanical properties of the tissue, such as its surface tension, are determined by cell-cell adhesion and cortical tension [31]. Recent work by Chiou *et al.* provides a method to measure the relative magnitude of forces acting within and between cells [32]. These results now make it possible to construct a quantitative cell-based tissue model in which wavefront propagation due to mechanical signaling can be studied as well.

Now that we have introduced a minimal model for mechanical signaling via nonlinear wavefront propagation, we can ask how one might identify biological contexts in which mechanical signaling is likely to occur. We can also ask how to determine whether a given wavefront is an example of mechanical signaling. Wavefronts of processes that generate stresses are obvious likely candidates. In order for a medium to be mechanically excitable, however, it is not enough to have a collection of nodes capable of generating stress. There must also be a mechanism to sense when a stress threshold is reached. Several such mechanisms have been identified [33], including stress-dependent ion channels that can release ions above a threshold stress [34–37], cell-cell adhesion complexes such as cadherin complexes [38], focal adhesions [39], and integrins [40]. Contractile wavefronts in heart tissue represent a good candidate for mechanical signaling [24]; cardiomyocytes generate stress as they contract via the excitation-contraction mechanism [41,42], and they sense stress as well—the contraction amplitude of a cardiomyocyte on a gel depends sensitively on the stiffness of the gel [24,43].

In addition, it is known that mechanical palpitation can disrupt contractile wavefronts [44]. Another possible realization is spreading cortical depression, which involves a potassium wavefront [5] that can be triggered mechanically [45]. These examples suggest that it may be worthwhile to reexamine nonlinear wavefronts in biological contexts to see if they are more properly interpreted as mechanical signaling.

ACKNOWLEDGMENTS

We thank Gareth Alexander, Michael Lampson, Tom Lubensky, and Phil Nelson for instructive discussions. This work was partially supported by the Netherlands Organization for Scientific Research through a Rubicon grant (T.I.) and by NSF-DMR-1104637 (T.I. and A.J.L.).

APPENDIX: EXPRESSIONS FOR THE GREEN'S TENSORS

1. Two-dimensional elastic model

In the simplest model that we consider, corresponding to a thin elastic film that slides frictionally over a surface, we balance the elastic force $\partial_j \sigma_{ij}$ with a friction term $\Gamma \partial_t u_i$, where Γ is the friction coefficient. Such a system can be described by a two-dimensional model with an equation of motion given by Eq. (2). The two-dimensional Green's tensor $G_{ijk}(\vec{x},t)$ associated with Eq. (2), relating the tensor Q_{ij} in a source term $\partial_j Q_{ij}\delta(\vec{x})\Theta(t)$ to an output u_k, is given by

$$G_{ijk}(\vec{x},t) = -\frac{1}{\mu x}\left\{\left[\left(\frac{1-\nu_2}{2}+\frac{8D_2t}{x^2}\right)e^{-x^2/4D_1t} - \left(1+\frac{8D_2t}{x^2}\right)e^{-x^2/4D_2t}\right]\frac{x_i x_j x_k}{x^3} - \frac{2D_2t}{x^2}[e^{-x^2/4D_1t} - e^{-x^2/4D_2t}]\phi_{ijk} + e^{-x^2/4D_2t}\delta_{ik}\frac{x_j}{x}\right\}, \tag{A1}$$

where $\mu = E_2/2(1+\nu_2)$, $D_1 = (2/(1-\nu_2))(\mu/\Gamma)$, $D_2 = \mu/\Gamma$, $x = \sqrt{\vec{x}\cdot\vec{x}}$, and $\phi_{ijk} = \delta_{ij}\frac{x_k}{x} + \delta_{ik}\frac{x_j}{x} + \delta_{jk}\frac{x_i}{x}$.

2. Three-dimensional two-fluid model

In the two-fluid model, we couple an elastic mesh, described by a displacement field u_i, to an incompressible viscous fluid, described by a velocity field v_i. The resulting equations are Eqs. (4)–(6), and the associated Green's tensor is given by

$$G_{ijk}(\vec{x},t) = G^{\text{hom}}_{ijk}(\vec{x},t) + G^{\text{stat}}_{ijk}(\vec{x},t), \tag{A2}$$

$$G^{\text{hom}}_{ijk}(\vec{x},t) = -\frac{1}{(2\pi x)^2 D_1\Gamma}\left[A\left(\frac{D_1t}{x^2}\right)\frac{x_i x_j x_k}{x^3} - B\left(\frac{D_1t}{x^2}\right)\phi_{ijk}\right] + \frac{e^{-t/\tau}}{(2\pi x)^2 D_2\Gamma}\left[A\left(\frac{D_2t}{x^2}\right)\frac{x_i x_j x_k}{x^3} - B\left(\frac{D_2t}{x^2}\right)\phi_{ijk}\right] - \frac{e^{-t/\tau}}{(2\pi x)^2 D_2\Gamma}C\left(\frac{D_2t}{x^2}\right)\frac{x_j}{x}\delta_{ik}, \tag{A3}$$

$$G^{\text{stat}}_{ijk}(\vec{x},t) = -\frac{2\pi(1+\nu)}{(2\pi x)^2 E}\delta_{ik}\frac{x_j}{x} - \frac{3(1+\nu)}{8\pi x^2 E(1-\nu)}\frac{x_i x_j x_k}{x^3} + \frac{(1+\nu)}{8\pi x^2 E(1-\nu)}\phi_{ijk} \tag{A4}$$

where $\mu = E/2(1+\nu)$, $D_1 = ((2-2\nu)/(1-2\nu))(\mu/\Gamma)$, $D_2 = \mu/\Gamma$, $\tau = \mu/\eta$, and

$$A(y) = \left(15\sqrt{\pi y} + \sqrt{\frac{\pi}{y}}\right)e^{-1/4y} + \left(\frac{3}{2} - 15y\right)\pi\,\text{erf}\left(\frac{1}{2\sqrt{y}}\right), \tag{A5}$$

$$B(y) = 3\sqrt{\pi y}e^{-1/4y} + \left(\frac{1}{2} - 3y\right)\pi\,\text{erf}\left(\frac{1}{2\sqrt{y}}\right), \tag{A6}$$

$$C(y) = \sqrt{\frac{\pi}{y}}e^{-1/4y} - \pi\,\text{erf}\left(\frac{1}{2\sqrt{y}}\right). \tag{A7}$$

For an input term that runs only over a time interval Δt as in Eq. (7) of the main text, continuity demands that for $t < \Delta t$ we have $G_{ijk}(\vec{x},t) = G^{\text{hom}}_{ijk}(\vec{x},t) + G^{\text{stat}}_{ijk}(\vec{x},t)$, and for $t > \Delta t$ we have $G_{ijk}(\vec{x},t) = G^{\text{hom}}_{ijk}(\vec{x},t) - G^{\text{hom}}_{ijk}(\vec{x},t-\Delta t)$.

[1] P. Devreotes, Science **245**, 1054 (1989).
[2] H. Levine and W. Reynolds, Phys. Rev. Lett. **66**, 2400 (1991).
[3] K. J. Lee, E. C. Cox, and R. E. Goldstein, Phys. Rev. Lett. **76**, 1174 (1996).
[4] J. D. Lechleiter and D. E. Clapham, Cell **69**, 283 (1992).
[5] N. A. Goroleva and J. Bures, J. Neurobiol. **14**, 353 (1983).
[6] G. H. Altman, R. L. Horan, I. Martin, J. Farhadi, P. R. H. Stark, V. Volloch, J. C. Richmond, G. Vunjak-Novakovic, and D. L. Kaplan, FASEB J. **16**, 270 (2001).
[7] D. E. Discher, P. Janmey, and Yu-li Wang, Science **310**, 1139 (2005).
[8] V. Vogel and M. Sheetz, Nat. Rev. Mol. Cell Biol. **7**, 265 (2006).
[9] D. E. Discher, D. J. Mooney, and P. W. Zandstra, Science **324**, 1673 (2009).
[10] S. D. Subramony, B. R. Dargis, M. Castillo, E. U. Azeloglu, M. S. Tracey, A. Su, and H. H. Lu, Biomaterials **34**, 1942 (2013).
[11] J. S. Bois, F. Jülicher, and S. W. Grill, Phys. Rev. Lett. **106**, 028103 (2011).
[12] X. Serra-Picamal, V. Conte, R. Vincent, E. Anon, D. T. Tambe, E. Bazellieres, J. P. Butler, J. J. Fredberg, and X. Trepat, Nat. Phys. **8**, 628 (2012).
[13] K. Kruse, J.-F. Joanny, F. Jülicher, J. Prost, and K. Sekimoto, Phys. Rev. Lett. **92**, 078101 (2004).
[14] K. Kruse, J.-F. Joanny, F. Jülicher, J. Prost, and K. Sekimoto, Eur. Phys. J. E **16**, 5 (2005).
[15] S. Günther and K. Kruse, New J. Phys. **9**, 417 (2007).
[16] S. Günther and K. Kruse, Chaos **20**, 045122 (2010).
[17] S. Banerjee and M. C. Marchetti, Soft Matter **7**, 463 (2011).
[18] S. Banerjee, T. B. Liverpool, and M. C. Marchetti, Europhys. Lett. **96**, 58004 (2011).
[19] M. Radszuweit, S. Alonso, H. Engel, and M. Bär, Phys. Rev. Lett. **110**, 138102 (2013).
[20] M. H. Köpf and L. M. Pismen, Soft Matter **9**, 3727 (2013).
[21] M. H. Köpf and L. M. Pismen, Physica D **259**, 48 (2013).
[22] M. C. Marchetti, J. F. Joanny, S. Ramaswamy, T. B. Liverpool, J. Prost, Madan Rao, and R. Aditi Simha, Rev. Mod. Phys. **85**, 1143 (2013).
[23] T. Idema, J. O. Dubuis, L. Kang, M. L. Manning, P. C. Nelson, T. C. Lubensky, and A. J. Liu, PLoS ONE **8**, e77216 (2013).
[24] S. Majkut, T. Idema, J. Swift, C. Krieger, A. J. Liu, and D. E. Discher, Curr. Biol. **23**, 2434 (2013).
[25] V. E. Foe and B. M. Alberts, J. Cell Sci. **61**, 31 (1983).
[26] F. de Jong, T. Opthof, A. A. Wilde, M. J. Janse, R. Charles, W. H. Lamers, and A. F. Moorman, Circ. Res. **71**, 240 (1992).
[27] L. D. Landau and E. M. Lifshitz, *Theory of Elasticity*, 3rd ed. (Butterworth Heinemann, Burlington, MA, 1986).
[28] T. Tanaka, L. O. Hocker, and G. B. Benedek, J. Chem. Phys. **59**, 5151 (1973).
[29] L. D. Landau and E. M. Lifshitz, *Fluid Mechanics*, 2nd ed. (Butterworth Heinemann, Burlington, MA, 1987).
[30] A. J. Levine and T. C. Lubensky, Phys. Rev. E **63**, 041510 (2001).
[31] M. L. Manning, R. A. Foty, M. S. Steinberg, and E.-M. Schoetz, Proc. Nat. Acad. Sci. USA **107**, 12517 (2010).
[32] K. K. Chiou, L. Hufnagel, and B. I. Shraiman, PLoS Comput. Biol. **8**, e1002512 (2012).
[33] C. C. DuFort, M. J. Paszek, and V. M. Weaver, Nat. Rev. Mol. Cell Biol. **12**, 308 (2011).
[34] P. G. Gillespie and R. G. Walker, Nature (London) **413**, 194 (2001).
[35] C. Kung, Nature (London) **436**, 647 (2005).
[36] C. Kung, B. Martinac, and S. Sukharev, Annu. Rev. Microbiol. **64**, 313 (2010).
[37] S. Sukharev and F. Sachs, J. Cell Sci. **125**, 3075 (2012).
[38] E. Tzima, M. Irani-Tehrani, W. B. Kiosses, E. Dejana, D. A. Schultz, B. Engelhardt, G. Cao, H. DeLisser, and M. A. Schwartz, Nature (London) **437**, 426 (2005).
[39] B. Geiger, J. P. Spatz, and A. D. Bershadsky, Nat. Rev. Mol. Cell Biol. **10**, 21 (2009).
[40] A. van der Flier and A. Sonnenberg, Cell Tissue Res. **305**, 285 (2001).
[41] H. E. Huxley, Science **164**, 1356 (1969).
[42] C. C. Ashley, I. P. Mulligan, and T. J. Lea, Q. Rev. Biophys. **24**, 1 (2009).
[43] A. J. Engler, S. Sen, H. L. Sweeney, and D. E. Discher, Cell **126**, 677 (2006).
[44] M. R. Franz, R. Cima, D. Wang, D. Profitt, and R. Kurz, Circulation **86**, 968 (1992).
[45] S. Akerman, P. R. Holland, and P. J. Goadsby, Brain Res. **1229**, 27 (2008).